Chapter 4: TaOx Nanodot Arrays

4.1 General Introduction

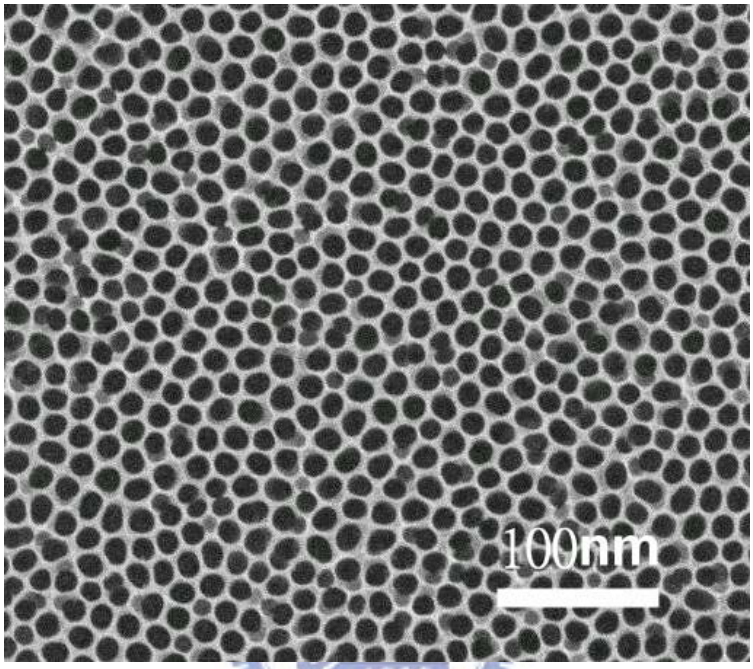

Figure 4-1 Top-view SEM image of the porous anodic alumina film anodizing after pore widening in 5-wt. % H_3PO_4.

The tantalum oxide nanodot arrays were carried out in three different electrolytes: 1.8M sulfuric acid, 0.3M oxalic acid and 0.5M phosphoric acid. According to previous records [1-9], each electrolyte suit to the specific applied voltage under the usual experimental conditions, the expansion of aluminum during oxidation leads to less than twice the original volume, but strongly depends on experimental conditions like the electrolyte concentration or anodizing voltage. Anodization was carried out in 1.8M sulfuric acid (under 5, 10, 15, 20, 25 and 30 constant polarization voltages), 0.3M oxalic acid (under 10, 20, 30, 40, 50 and 60 constant polarization voltages) and

5wt-% phosphoric acid (under 100 constant polarization voltages). In our approach, we not only seek for ordered nanodot arrays but reducing on the scale of nanodots. Figure 4-1 shows the top-view scanning electron microscopy (SEM) image of the porous anodic alumina film anodizing in 0.3M oxalic acid at 40V after pore widening in a 5% H_3PO_4 solution at room temperature for 2hr. The self-organized nanopores with a uniform size distribution have a pore diameter about 60 nm and an interpore distance about 100 nm. The anodic alumina pores do not show a long-range order, but within a pore array domain. It may be possible to obtain more ordered pores with a narrower size distribution by starting with thicker and fine quality films [1].

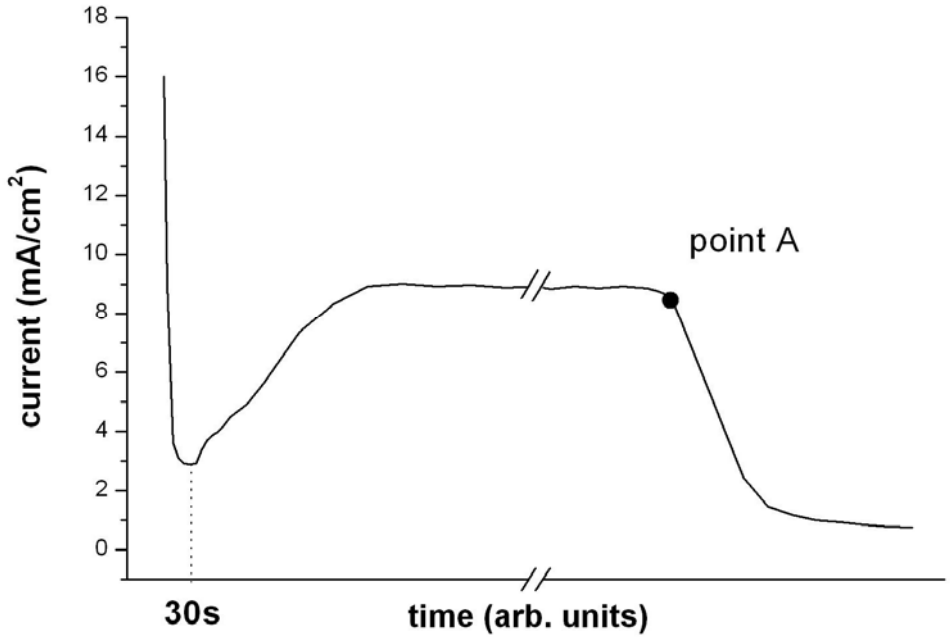

Figure 4-2 Current versus time plots produced during the anodization of aluminum films of sample J.

We recorded the current versus anodization time to figure out the process

exhaustively. All current-versus-time plots have the same appearance but different intensity in x and y axis. We took sample J (oxalic in 40V) as an example and presented current versus anodization time plot in Figure 4-2. The current started high, decreased as an oxide layer was formed on the surface and tantala nuclei was appeared simultaneously. The current reached to a steady level as the pores began to propagate through the alumina and accompanied the growth of the tantala nucleus. When the porous alumina films on the substrate had been nearly completely anodized, there was a distinct color change resulting from the transparency of the porous alumina. At this point (point A in Figure 4-2), the current reduced and growth of the nanodot terminated. The period of the steady level depended on the thickness of aluminum film and the reaction temperature. There is a longer duration of the steady level for thicker aluminum films or lower temperature. It is believe that the growth of the nanodot terminated when the porous alumina completed because of the same diameter of nanodot of different anodic time and cut-off current under the constant voltage. Additionally, in higher electric field the electrolyte may directly penetrate between the top of the nanodot because of the breakage of the barrier layer by violent expansion of oxidation of nanodot. It was allowed further direct oxidation and evolution of the nanostructure to their final shape more like nanorod [10] after a period of anodic time. One way to obtain highly ordered arrays of nanodot is starting with fine quality aluminum films.

4.2 Oxalic and Sulfuric acid Specimen

4.2.1 Morphology of Nanodot Arrays

The top-view SEM images of the tantalum oxide nanodot arrays formed in various applied voltage and two different electrolytes after removing the overlying alumina film are shown from Figure 4-3 to Figure 4-6. Two electrolytes have been

selected because of the difference in the forming voltages and electrolyte-derived species, which affected the properties of the nanodots. The population density and average diameter of nanodot were calculated and plotted in Figure 4-7. The nanodot diameter ranges between 10nm ~ 70nm and density ranges between $10^{11}/cm^2$ ~ $10^{10}/cm^2$. The performance of the reduction in dimension and high density is superior to other reports [11-13]. The diameter and density of the nanodot can be controlled by various applied voltages. Regardless of the electrolyte, the distances between nanodots tend to be proportional to the anodizing voltages with constant of 2.5nm/V [14]. We also calculated the average distance between nanodots' center and average gap width between nanodots' bases of tantalum oxide nanodots, and plotted in Figure 4-8. The average distance between nanodots' center versus anodic voltage in self-organized porous alumina is in common with the relation d=-1.7+2.81Ua [15], which d represents the interpore distance and Ua is for sulfuric, oxalic, and phosphoric acid solutions. In oxalic acid specimen, the orders of the nanodot arrays in low applied voltage reduce and tended to small domain which only contained several nanodots. Moreover, the shape of nanodot bases in oxalic acid specimen distorted fiercely and deformed in unregulated. In sulfuric acid specimen, the distance between nanodot bases is smaller than oxalic acid specimens in same applied voltage, that is, the diameter of nanodot in sulfuric acid specimen is larger than oxalic acid specimens under the same applied voltage. The order of nanodot arrays had better performance in low applied voltage. The best orders of nanodot arrays in oxalic acid specimen is 40~50V while 20~30V in sulfuric acid specimen.

Sub-10nm diameter, 3nm gap width and 4×10^{11} density nanodot arrays can be fabricated in the novel method of this thesis, and have a great potential for quantum phenomenon application. It seems that smaller nanodot can be fabricated by lower applied voltage, but we suppose that there is a limitation of the minimum of anodic

nanodot on account of the tendency in Figure 4-7 and insufficient electric field of anodization. The average diameter of self-organized nanodot arrays of tantalum oxide is relatively larger than the corresponding pore size of the alumina film without pore-widening. It may be due to the radial anodizing field distribution at the Ta layer. The densities of tantalum oxide nanodot were in good agreement with the pore density of the pores of anodic alumina. Figure 4-6 (A) shows the SEM image of a cross-section of the nanodot in oxalic acid at 40V, and it proved that the nanodot was formed under the bases of corresponding alumina pores while after removing the porous alumina film in Figure 4-6 (B). Horizontal projections of the bases look like distorted hexahedrons. During nanodots growth the ionic current is distributed unevenly across the barrier layer, concentrating along nanometer sub-channels, which merge inside the hillocks and result in appearance of the root-like structure and distorted hexagonal bases of the nanodots formed. Note that some tiny bulges appeared on nanodots result from the aggregation of the Pt thin film which increased the electric conductivity under SEM.

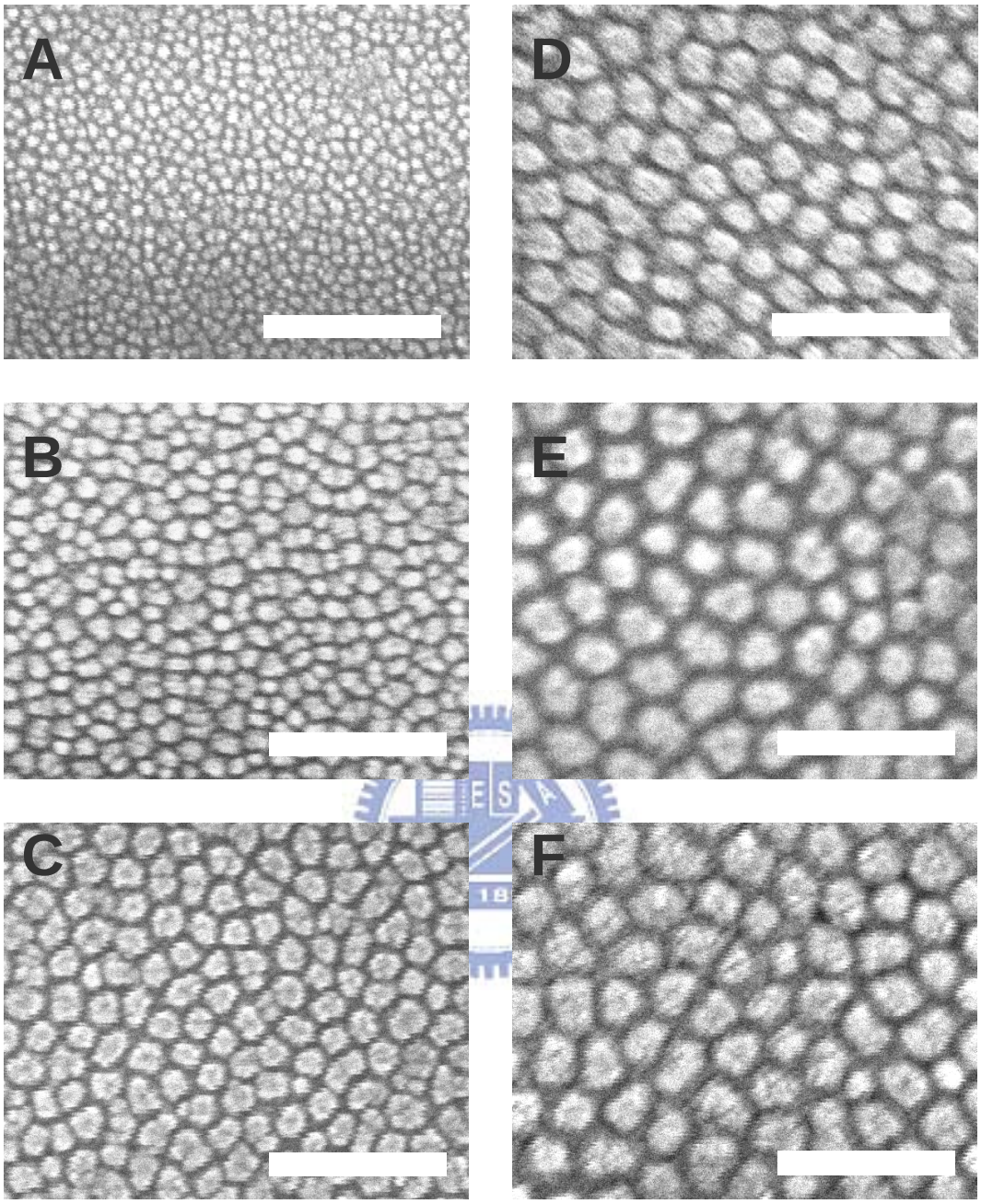

Figure 4-3 SEM images of tantalum oxide nanodot arrays in 1.8M sulfuric acid at (A) 5V (B) 10V (C) 15V (D) 20V (E) 25V (F)30V . The scale bar is 100 nm.

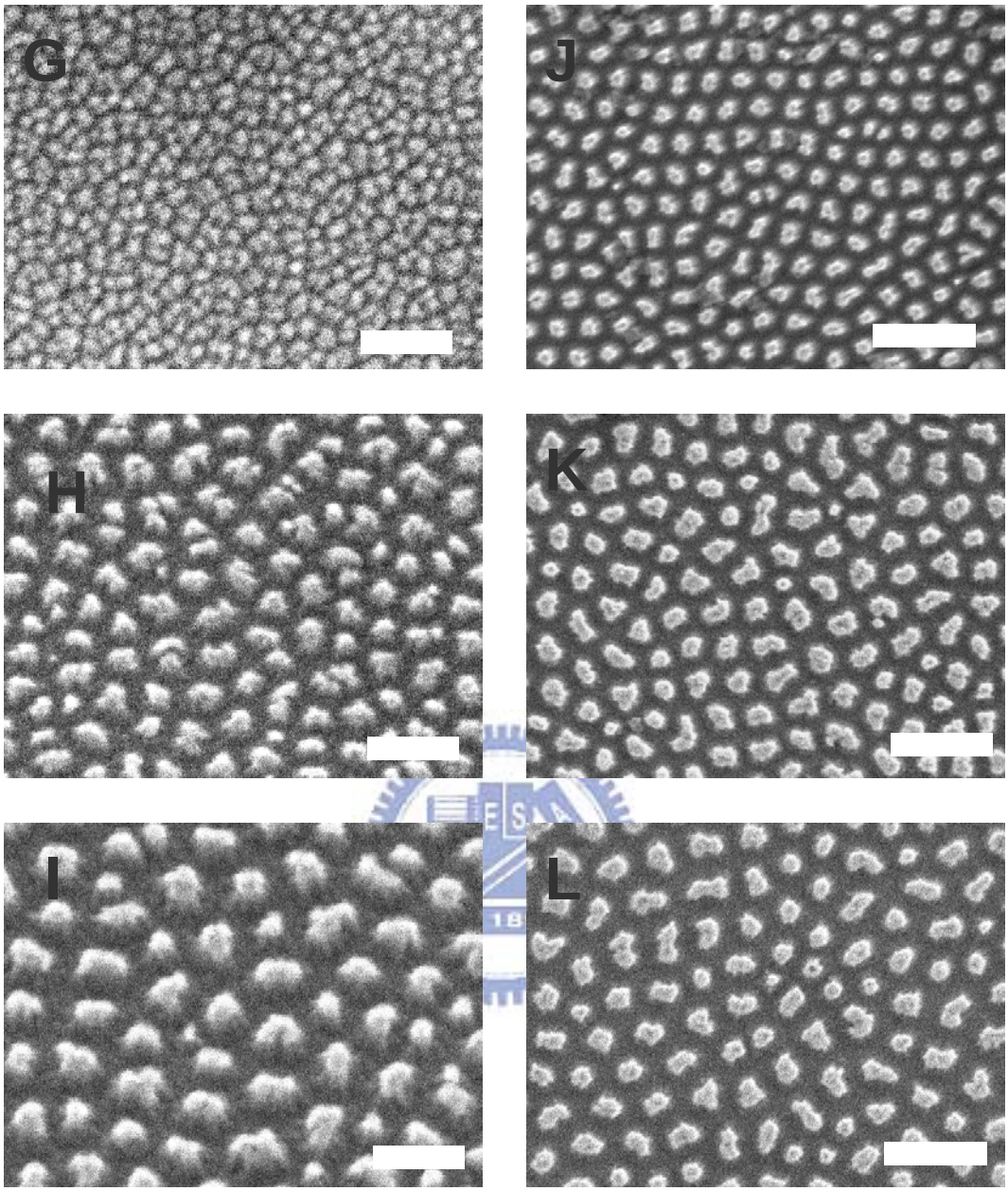

Figure 4-4 SEM images of tantalum oxide nanodot arrays in 0.3M oxalic acid at (G) 10V (H) 20V (I) 30V. The scale bar is 100 nm. (J) 40V (K) 505V (L) 60V. The scale bar is 300 nm.

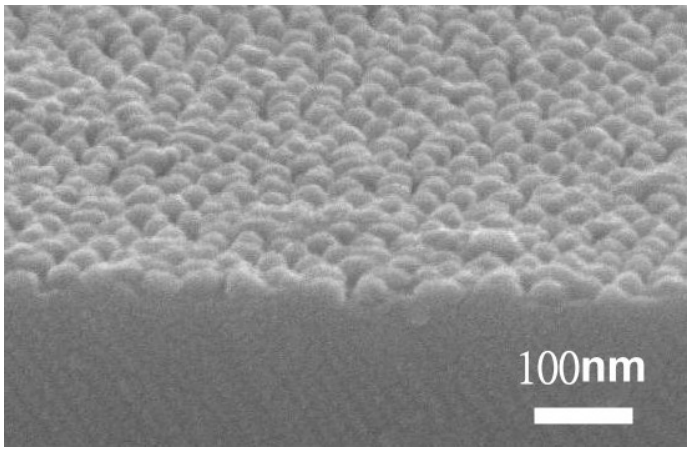

Figure 4-5. Slide-view SEM image of tantalum oxide nanodots arrays on the surface of sample J.

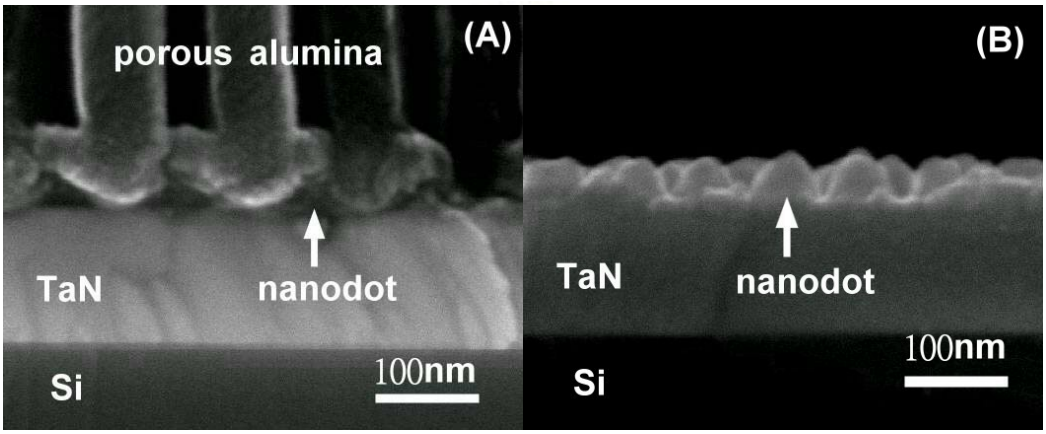

Figure 4-6 (A) cross-section SEM image of the nanodots with overlying porous alumina film, (B) after removing alumina film.

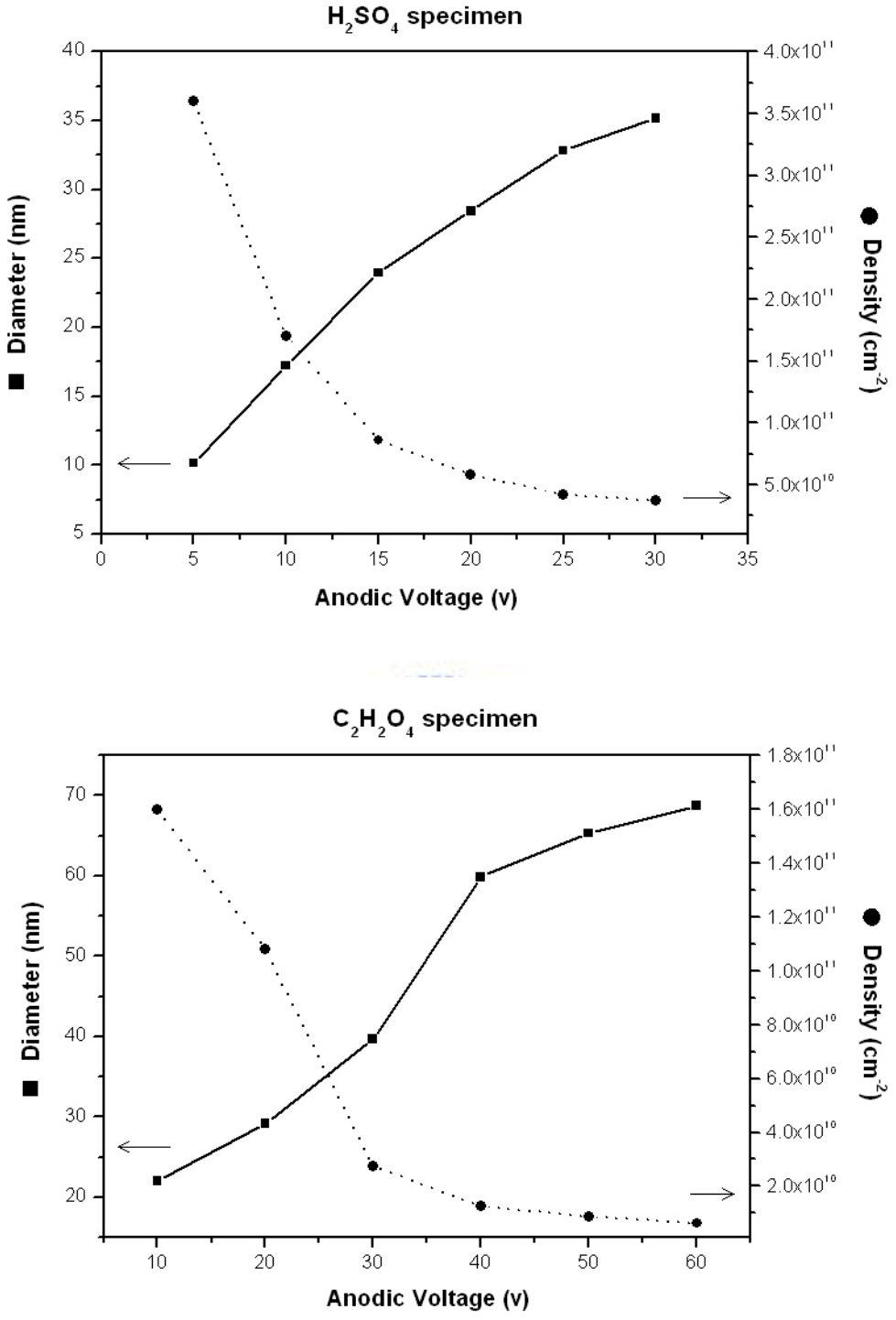

Figure 4-7 The effect of applied voltage on average diameter and density of tantalum oxide nanodots. (A) H_2SO_4 specimen. (B) $H_2C_2O_4$ specimen.

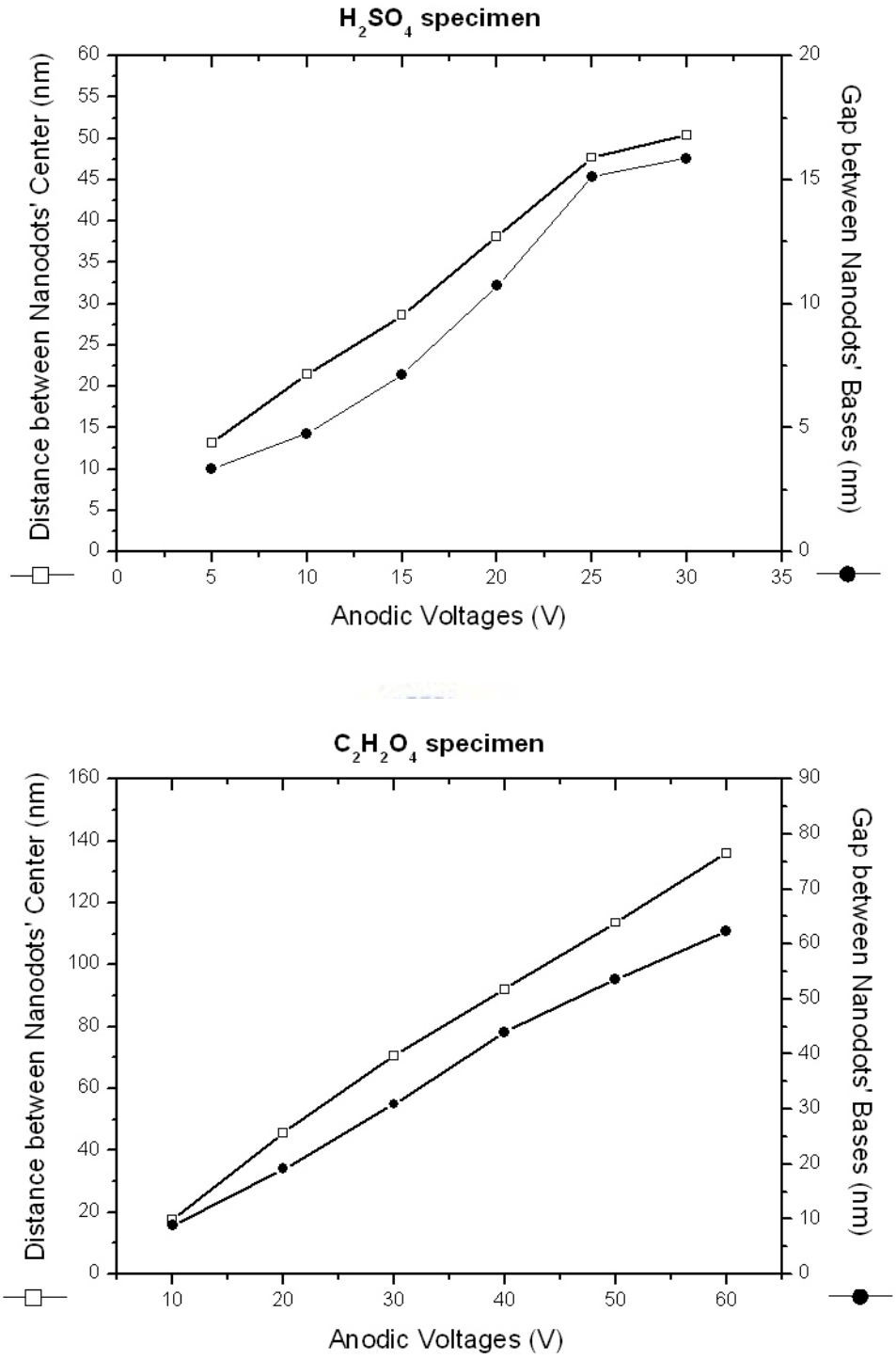

Figure 4-8 The effect of applied voltage on average distance between nanodots' center and average gap width between nanodots' bases of tantalum oxide nanodots. (A) H_2SO_4 specimen. (B) $H_2C_2O_4$ specimen.

4.2.2 Mechanism of Growth of Nanodot Arrays

The anodization behavior of the Ta/Al film on the silicon wafer is different from the case of the Al film directly deposited on semiconductor substrates or foil aluminum. In the first instance, the above aluminum layer oxidized to alumina, accompanied by the outward migration of Al^{3+} and inward diffusion of O^{2-} driven by the applied electric field, leading to the vertical pore channel growth. Furthermore, the bottom of the alumina film consisted of an array of convex hemispheres during the initial anodization, and the position of nanodot had been decided. The alumina dissolution at the alumina /electrolyte interface is in equilibrium with the alumina growth at the Al/Al_2O_3 interface. As the oxide barrier layer at the pore bottom approaches the Ta/Al interface, the O^{2-} migrating inwards through the alumina barrier layer are continuously injected into the Ta layer and form the tantalum oxide. The O^{2-} released from the dissociated barrier layer at the Ta_2O_5/ Al_2O_3 interface are also injected into the Ta_2O_5 layer, while the released Al^{3+} migrate outwards through the remaining barrier layer and are mostly expelled in the electrolyte. The O^{2-} injected into the Ta_2O_5 layer then migrate inwards and the Ta layer is anodized normally to form new oxide at the Ta/Ta_2O_5 interface. In brief, the underlying tantalum oxide by O^{2-} transported through/from the barrier layer of the initially formed porous alumina without direct contact of Ta with the electrolyte. The tantalum oxide nanodot resulting from oxidation of the Ta layer is accompanied by a volume expansion. Eventually, the aluminum completely transferred into alumina accompanied the end of the all anodic process. During nanodots growth the ionic current is distributed unevenly across the barrier layer, concentrating along nanometer sub-channels, which merge inside the hillocks and result in appearance of the root-like structure and distorted hexagonal bases of the nanodots formed.